Heliyon 7 (2021) e06006

Contents lists available at ScienceDirect

Heliyon

journal homepage: www.cell.com/heliyon

Research article

Evaluation of *TH*-Cre knock-in cell lines for detection and specific targeting of stem cell-derived dopaminergic neurons

Alessandro Fiorenzano [*], Marcella Birtele, Jenny Nelander Wahlestedt, Malin Parmar [**]

Developmental and Regenerative Neurobiology, Wallenberg Neuroscience Center, And Lund Stem Cell Centre, Department of Experimental Medical Science, Lund University, 22184 Lund, Sweden

ARTICLE INFO

Keywords:
Human pluripotent stem cells
Dopamine differentiation
Parkinson's disease
Cell transplantation

ABSTRACT

The focal and progressive degeneration of dopaminergic (DA) neurons in ventral midbrain has made Parkinson's disease (PD) a particularly interesting target of cell-based therapies. However, ethical issues and limited tissue availability have so far hindered the widespread use of human fetal tissue in cell-replacement therapy. DA neurons derived from human pluripotent stem cells (hPSCs) offer unprecedented opportunities to access a renewable source of cells suitable for PD therapeutic applications. To better understand the development and functional properties of stem-cell derived DA neurons, we generated targeted hPSC lines with the gene coding for Cre recombinase knocked into the *TH* locus. When combined with flexed GFP, they serve as reporter cell lines able to identify and isolate TH^+ neurons *in vitro* and after transplantation *in vivo*. These *TH*-Cre lines provide a valuable genetic tool to manipulate DA neurons useful for the design of more precise DA differentiation protocols and the study of these cells after transplantation in pre-clinical animal models of PD.

1. Introduction

The degeneration of dopaminergic (DA) neurons in ventral midbrain (VM) is known to play a key role in the development of Parkinson's disease (PD). Attempts to design a cell therapy for PD based on replacing cells lost to the disease with new healthy DA neurons have spanned more than three decades [1]. Early trials using fetal VM tissue provided proof-of-concept that such an approach can be effective in slowing disease progression. However, the limited availability of fetal tissue as well as ethical and practical complications associated with its use have hampered the advancement of this therapeutic strategy and pointed to the need to identify alternative cell sources [2]. Human pluripotent stem cells (hPSCs) are widely expected to provide an alternative donor cell population available in unlimited quantities, and global efforts to use hPSC-derived DA neurons in PD patients are ongoing [3,4].

Previous experimental studies showed the function and innervation of stem cell-derived DA neurons in pre-clinical models of PD [5,6,7,8,9]. To further refine such studies and to track DA neurons during *in vitro* differentiation, we generated targeted cell lines with the gene coding for Cre recombinase knocked into the *TH* locus. When combined with flexed GFP, they serve as reporter cell lines allowing for the identification and isolation of TH neurons *in vitro* and after transplantation *in vivo*. These *TH*-Cre lines also provide a robust and flexible genetic tool to manipulate DA neurons such as by inserting designer receptors exclusively activated by drugs (DREADDs) or channelrhodopsins for the specific activation or inhibition of DA neurons, or by performing rabies-based tracing from transplanted DA neurons.

The ability to detect and specifically target DA neurons will represent a crucial step forward in the continuous efforts to design more precise DA differentiation protocols and to study these cells after transplantation in pre-clinical animal models of PD.

2. Results

2.1. Generation and validation of CRISPR/Cas9-mediated TH-Cre knock-in reporter cell lines

To knock Cre recombinase into the *TH* locus, we designed two different targeting approaches. One was based on knocking Cre into exon 1 of the *TH* gene (Figure 1A), which has three isoforms (-001, -002, and -003) sharing the same start codon in exon 1. The other mimicked a previously reported *TH*-Cre rat model [10], with the additional insertion

* Corresponding author.
** Corresponding author.
E-mail addresses: alessandro.fiorenzano@med.lu.se (A. Fiorenzano), malin.parmar@med.lu.se (M. Parmar).

https://doi.org/10.1016/j.heliyon.2021.e06006
Received 13 July 2020; Received in revised form 21 October 2020; Accepted 12 January 2021

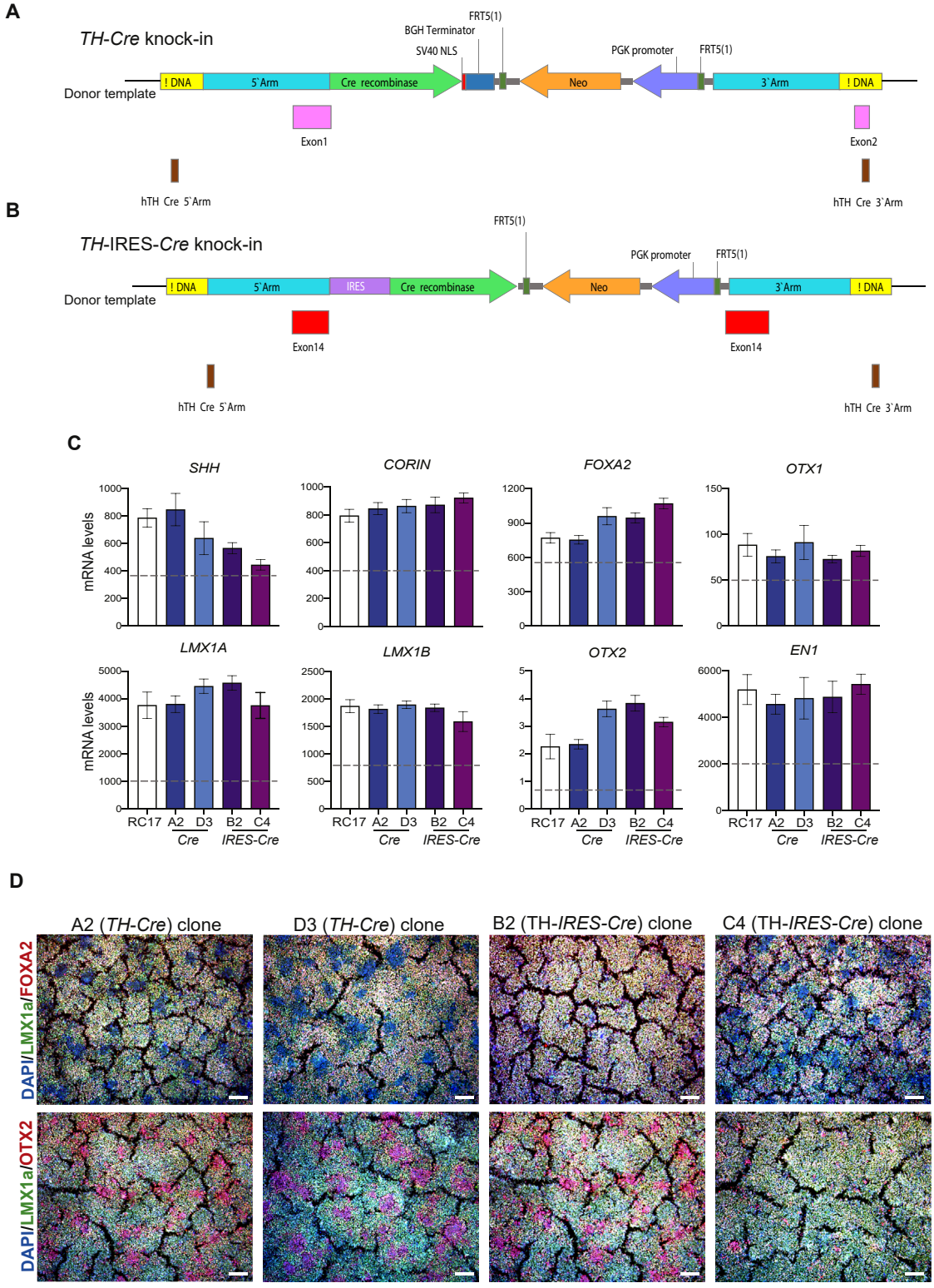

Figure 1. A, Schematic overview of targeting strategies to knock Cre into exon 1 B, or IRES-Cre into 3′UTR of human *TH* gene. C, qRT-PCR of selected markers at day 16 of cells patterned toward ventral midbrain (VM). Results are given as fold change over undifferentiated hPSCs. Data represent mean ± SEM of 3 independent experiments. Dotted line show range used to determine successful midbrain patterning. D, Immunohistochemistry of LMX1a/FOXA2 and LMX1a/OTX2 at day 16 in Cre-targeted hPSC clones (A2 and D3), and of IRES-Cre targeted hPSC clones (B2 and C4) patterned toward VM. Scale bars, 100 μM. Nuclei were stained with DAPI.

of an internal ribosomal entry site (IRES)-Cre cassette in exon 14 [11] (Figure 1B). Targeting of the donor templates was achieved using specific guide RNAs and CRISPR/Cas9 technology. We verified the correct insertion at both the 5′ and 3′ ends by PCR genotyping (Supplementary Fig. 1A,D). We used primer pairs binding outside TH donor vector homology arms and a second primer binding within sequences not contained in wild-type cells, thereby distinguishing targeted clones from those with random genomic insertions (Supplementary Fig. 1A,D and

Supplementary Table1). DNA sequencing of PCR products confirmed precise insertion of the reporter gene (4/12 clones screened from *TH*-Cre reporter and 7/18 clones screened from IRES-Cre knock-in cell lines), indicating that genomic editing was efficiently targeted to the *TH* locus (Supplementary Fig. 1C,F). To determine whether the insertion was present in one or both alleles, PCR genotyping was used to distinguish the wild-type from the modified allele and we found that *TH*-Cre and IRES-Cre knock-in clones were heterozygous and homozygous for the insertion, respectively (Supplementary Fig. 1B,E and Supplementary Table 1).

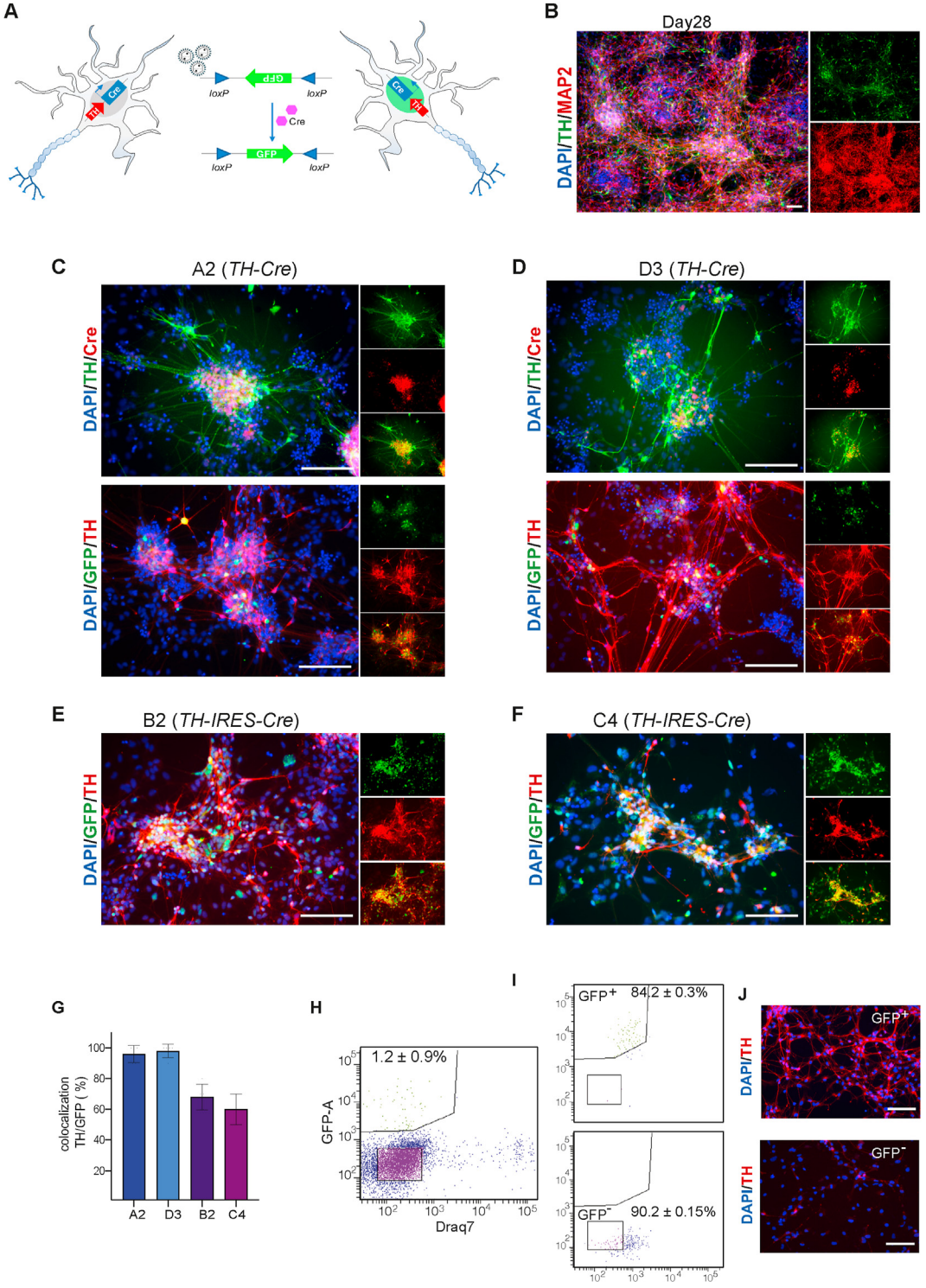

Figure 2. A, Schematic representation of FLEx-GFP in *TH*-Cre reporter cell line. B, Immunohistochemistry of TH/MAP2 in A2 clone at day 28 during VM differentiation. Scale bars, 100 μM. Nuclei were stained with DAPI. C, Immunohistochemistry of TH/CRE and GFP/TH in A2 and D, in D3 *TH*-Cre targeted hPSC clones at day 28 during VM differentiation. Scale bars, 250 μM. Nuclei were stained with DAPI. E, Immunohistochemistry of TH/CRE and GFP/TH in B2 and F, in C4 *TH*-IRES-Cre targeted hPSC clones at day 28 during VM differentiation. Scale bars, 250 μM. Nuclei were stained with DAPI. G, Quantification (%) of GFP^+ cells co-expressing TH in *TH*-Cre-targeted hPSC clones (A2 and D3) and IRES-Cre hPSC clones (B2 and C4) at day 28 during VM differentiation. H, FACS-based separation and I, post-sorting analysis of VM progenitor GFP^+ and GFP^- cells. Data represent mean ± SEM ($n = 3$). J, Immunohistochemistry of TH in GFP^+ and GFP^- FACS- separated cells.

Based on these findings, we identified and selected two correctly targeted clones from the *TH*-Cre (A2 and D3) and the *TH*-IRES-Cre (B2 and C4) design for further analysis (Supplementary Figure 1A,B,D,F). To assess if genome modification of the targeted *TH* locus impacted the ability of hPSCs to differentiate, we induced these four clones to DA progenitors following a well-established protocol [12,13]. The ventral and caudal midbrain patterning of these *TH*-Cre and *TH*-IRES-Cre targeted clones was compared to that of the parental cell line differentiated in parallel. We confirmed correct VM patterning by performing qPCR for key genes (*SHH, CORIN, FOXA2, OTX1, LMXA1, LMX1B, OTX2,* and *EN1*) that was all in the range of our QC criteria [13] (Figure 1C and Supplementary Table 2) and by assessing co-expression of LMX1a/-FOXA2 and LMX1A/OTX2 at protein level (Figure 1D). Western blot analysis confirmed that the level of TH expression was not significantly different between the two targeting strategies (Supplementray Figure 2A). Taken together, these findings indicate that knock-in of Cre in *TH* locus does not alter the developmental potential of targeted cells to differentiate.

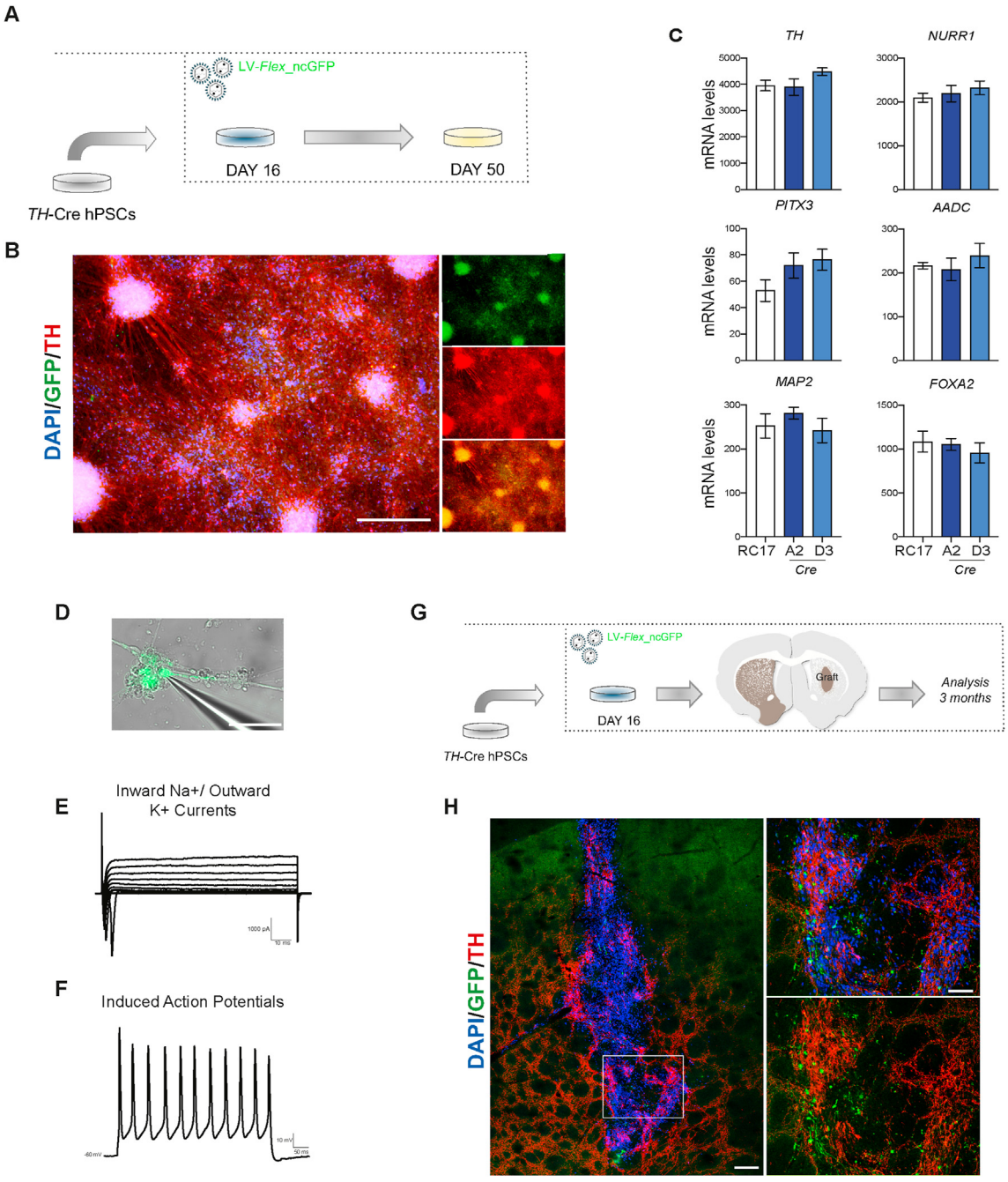

Figure 3. A, Schematic overview of *in vitro* experimental plan. B, Representative qRT-PCR of selected markers at day 50 of terminally differentiated VM cells. Results are given as fold change over undifferentiated hPSCs. Data represent mean ± SEM of 3 independent experiments. C, Immunohistochemistry of TH/GFP of A2 *TH*-Cre targeted hPSC clone at day 50 during VM differentiation. Scale bars, 250 μM. Nuclei were stained with DAPI. D, Bright field image representing whole-cell patch-clamp recordings of GFP^+ cells. Scale bars, 100 μM. E, Representative trace of inward sodium- and outward potassium-rectifying current traces in GFP^+ cells triggered by stepwise depolarization. F, Representative trace of induced action potentials triggered upon stepwise current injection. G, Schematic overview of in *vivo* experimental plan. H, Immunohistochemistry of TH/GFP in the graft core of VM-derived hPSC intrastriatal grafts 3 months post-transplantation. Insets show high-power magnifications of GFP^+ DA neurons in the graft. Scale bars, 200 μM. Nuclei were counterstained with HUNU.

2.2. GFP is specifically expressed in TH neurons in TH-Cre knock-in reporter lines when transduced with cre-activatable reporter construct

To test the ability of selected transgenic hPSC-reporter cell lines to detect DA neurons in live cultures, we transduced the cells with a Cre-inducible (DIO, or double-floxed inverted orientation) GFP expression cassette in undifferentiated hPSCs (Supplementary Fig. 2B). The specificity of flip-excision (FLEx)-GFP to TH^+-expressing cells and the off-target function of this vector was first tested at protein level in undifferentiated hPSC culture. FACS and immunofluorescence analysis detected no ectopic expression of GFP in absence of Cre (Suppl. Fig. 2C,E) when transgenic lines were transduced with FLEx-GFP virus alone. In contrast, when hPSCs were co-transduced with both Cre and FLEx-GFP lentivirus, GFP was only detected in Cre-expressing cells (Supplementary Fig. 2F,D). We then analyzed the expression of TH, Cre, and GFP at day 28 after initiation of DA differentiation (Figure 2A), at a timepoint when many cells had acquired a neuronal phenotype as detected by MAP2 expression (Figure 2B). Immunofluorescence showed that Cre and GFP expression co-localized with TH (Figure 2C,D), confirming that TH and GFP are specifically co-expressed in both clones from the *TH*-Cre knock-in (Figure 2C–D). By contrast, in the IRES-Cre line, GFP was found expressed both earlier and more broadly than TH in both independent B2 and C4 clones (Figure 2E,F). Quantifications of GFP and TH co-localization confirmed this observation (Figure 2G). We therefore focused the remainder of our analysis on the *TH*-Cre knock-in clones. We further differentiated these selected hPSC reporter lines into DA progenitors and used FACS to enrich TH^+ cells in culture (Figure 2H). Based on GFP expression, we sorted and collected GFP^+ and GFP^- cells, and then analyzed TH expression after 12 h (Figure 2I,J). Dead cells were excluded by DRAQ7 staining (Supplementary Fig. 2G,H). Immunofluorescence analysis confirmed that most TH neurons were recovered from the GFP^+ cell population (Figure 2J).

2.3. TH-cre reporter cell line allows the study of developing and functionally mature DA neurons

To further investigate whether mature DA neurons can be detected using the *TH*-Cre reporter cell line, we tested the persistence of GFP expression in terminally differentiated DA neurons cells by performing long-term *in vitro* and *in vivo* experiments (Figure 3A-H). We transduced *TH*-Cre cells with LV-FLEx-ncGFP at DA progenitor state (day 12; MOI = 2) and subsequently differentiated them *in vitro* until day 50 (Figure 3A and Supplementary Fig. 2I). GFP was detected in live cultures (Supplementary Fig. 2J) and overlap with TH was confirmed on day 50 by immunocytochemical staining on fixed cells (Figure 3B and Supplementary Fig. 2K). Gene expression analysis for *TH*, *NURR1*, *PITX3*, *AADC*, *MAP2*, and *FOXA2* (Figure 3C and Supplementary Table2) confirmed proper DA differentiation patterning. We next performed whole-cell patch-clamp recordings to assess functional maturation of GFP-labeled cells. The targeted GFP^+ cells exhibited hyperpolarized resting membrane potentials (-49mV), and inward sodium (Na^+) - outward delayed-rectifier potassium (K^+) currents indicative of a neuronal state (Figure 3D,E). Also, the ability to fire induced action potentials (APs) upon current injections was indicative of a mature neuronal function (Figure 3F). Using a similar strategy but with a nuclear GFP reporter (Figure 3G), we transplanted day 16 progenitors into the striatum of 6-OHDA lesioned nude rats and then analyzed the cells 3 months after grafting by immunohistochemistry (Figure 3H). This analysis corroborated that ncGFP is maintained also in mature TH neurons after grafting.

3. Discussion

Here we describe the establishment of hPSC reporter lines where Cre is knocked into exon 1 of the *TH* gene. Using viral vectors where GFP and ncGFP (DOI) are transduced into pluripotent and/or progenitor cells, we showed that this design results in the expression of GFP selectively in TH^+-expressing neurons *in vitro* and after transplantation *in vivo*. In this *TH*-Cre reporter line, targeting disrupts the *TH* gene and TH is only expressed from one allele. We also tested an alternative approach based on a *TH*-Cre rat model [10] with the additional insertion of an IRES-Cre cassette in 3′UTR. This transgenic reporter line has the advantage that the endogenous *TH* gene is not disrupted and that a homozygous Cre knock-in is possible if high Cre levels are required. Although this design works well in rats [7,10], we found some leakage of expression outside TH^+ neurons in stem cell cultures.

Knocking Cre into the gene locus instead of following the more conventional strategy of inserting a specific fluorescent reporter [14] presents several advantages. *Firstly*, it allows for greater flexibility in the choice of reporter. Here we describe the use of GFP, which is useful when studying DA neurons *in vitro* or assessing morphology and projections *in vivo*, and of ncGFP, which can also be used for live-cell imaging, facilitates quantification, and allows for cell/nuclei sorting after transplantation has been performed with ubiquitously expressed GFP [15]. For other applications, any type of reporter could be inserted as required. Live reporters in DA neurons can also be used in more advanced techniques such as scRNAseq and Patch-seq analysis in order to combine assessment of genome-wide expression with neuronal activity and morphological characterization, thus facilitating the functional classification and mapping of DA neuronal subtypes. *Secondly*, many types of construct could be incorporated and used to refine *in vivo* studies where specifically targeting and studying the DA component of grafts is challenging [5,6,16]. *Thirdly*, the *TH*-Cre line can be adopted to selectively regulate DA neuron function in a bimodal manner, as previously performed with transplanted rat cells [7]. A drawback of Cre-based reporter design is that it requires efficient targeting of the reporter construct in order to activate expression in TH^+ cells. In this study, we use the lentiviral delivery system that results in highly efficient targeting *in vitro*. For other studies, for example when delivery *in vivo* is required, other vector systems need to be used and optimized for each application.

We envision that this *TH*-Cre reporter cell line will serve as a valuable tool to refine stem cell differentiations and to better understand the functions and properties of DA neurons after transplantation.

4. Methods

4.1. hPSC culture

Undifferentiated RC17 (Roslin Cells, #hPSCreg RCe021-A) and *TH*-Cre hPSC cells were maintained on 0.5 μg/cm^2 Laminin-521 (Biolamina, #LN-521)-coated plates in iPS Brew medium (Miltenyi, #130-104-368).

4.2. Generation of TH-Cre and TH-IRES-Cre hPSC lines

The Cre-recombinase sequence was inserted in exon 1 of the TH gene, in frame and downstream of ATG, right after ATG, and followed by stop codon-loxp-PGK-puro-loxp. For this purpose, gRNAs were designed to target intron 1. Among the gRNA candidates, one of them was selected based on the proximity to the target site and off-target profiles: MS405.TH.g38 (5′-CACATCCACGCCGCGTCCCAGGG-3’; in bold is reported Protospacer Adjacent Motif (PAM) site). The selected gRNAs were cloned into a gRNA/Cas9 expression vector by inserting double-stranded oligo cassettes of their DNA sequences between the two Bbs I sites. gRNA constructs were verified by RE digestion and sequencing. After the double-stranded oligos of the two gRNAs were cloned into the gRNA expression vector pBTU6-Cas9-2A-GFP, each construct was transfected into K652 cells individually. Genomic DNA was extracted and PCR was performed (5′-GTGTCTGAGCTGGACGCC-3’; 5′-GATTCAAGATGAAACAAGACA-CAG-3′). The PCR products were subjected to NGS to assess the frequency of NHEJ events that result from DSB at the HT locus. The cells RC17 cells were transfected with the gRNA MS405.TH.g38 and the donor plasmid. After a 2-week puromycin selection, clones were isolated and genotyped.

For TH-IRES-Cre, IRES-Cre was knocked into UTR of TH gene following the design of the transgenic rat [10]resulting in cre expression

whenever the TH promoter is activated, and that the TH gene also will be fully translated.

4.3. hPSC differentiation

RC17 and *TH*-Cre hPSC cells were differentiated into VM-patterned progenitors using our GMP-grade protocol [13]. VM-patterned progenitors were either transplanted after 16 days of differentiation or were replated on day 16 as described [13] and kept in culture until day 50 of differentiation. For nuclear expression of GFP, *TH*-Cre hPSC cells (passage 10) were transduced with a lentiviral construct under control of the human *TH*-Cre promoter (Addgene, plasmid). The cells were transduced at a multiplicity of infection (MOI) of 1 while cultured on Laminin-521 in iPS-Brew.

4.4. Flow cytometry

TH-Cre hPSC and *TH*-Cre VM-patterned single cell suspensions were obtained using Accutase. After dissociation, the cells were analyzed and sorted by FACS based on GFP expression using a BD FACSAria III Cell Sorter (BD Biosciences).

4.5. Animals

Athymic nude female rats (180 g) were purchased from Harlan laboratories (Hsd:RH-Foxn1$_{rnu}$) and housed in individual ventilated cages under a 12:12 h dark-light cycle with *ad libitum* access to sterilized food and water. All procedures on research animals were performed in accordance with the European Union Directive (2010/63/EU) and approved by the local ethical committees at Lund University and the Swedish Board of Agriculture (Jordbruksverket). For all surgical procedures, rats (minimum 225 g/16–18 weeks) were anesthetized via i.p. injection using a 20:1 mixture of fentanyl-dormitor (Apoteksbolaget). The animals were rendered hemiparkinsonian via unilateral injection of 4 μL of the neurotoxin 6-hydroydopamine at a concentration of 3.5 μg/μL (calculated from free-base HCl) aimed at the following stereotaxic coordinates (in mm): anterior -4.4, medial -1.2, and dorsal -7.8, with the incisor bar set at 2.4. Injections were performed as described [17] at an injection speed of 1 μL/min with an additional 3 min allowed for diffusion before careful retraction of the needle. Intrastriatal transplantation was performed by injecting a total of 300,000 hESC-derived VM-patterned cells resuspended in 4 μL over four 1 μL deposits (75,000 cells per deposit) at the following coordinates relative to bregma (in mm): anterior +1.2, medial -2.6, dorsal -4.5 and -4.0 and anterior +0.5, medial -3.0. At each deposit the injection cannula was left in place for an additional 2 min before careful retraction to allow for settling of the tissue. Rats were transcardially perfused using 50 mL physiological saline solution (8.9% saline) for 1 min followed by 250 mL 4% paraformaldehyde (PFA, pH 7.4) solution for 5 min.

4.6. qRT-PCR

Total RNAs were isolated using the RNeasy Micro Kit (QIAGEN, #74004) and reverse transcribed using random hexamer primers and Maxima Reverse Transcriptase (Thermo Fisher, #K1642Invitrogen). cDNA was prepared with SYBR Green Master Mix (Roche, #04887352001) using the Bravo instrument (Agilent) and analyzed by quantitative PCR on a LightCycler 480 supplier using a 2-step protocol with a 60 °C annealing/elongation step. All quantitative reverse transcriptase PCR (qRT-PCR) samples were run in technical triplicates and results are given as fold change over undifferentiated hPSCs. Details and list of primers are reported in Supplementary Table 1.

4.7. Immunocytochemistry

Terminally differentiated cell cultures (day 50) were fixed in 4% PFA for 15 min and then washed three times with PBS. For immunocytochemistry, the cells were blocked for 1–3 h in PBS +5% donkey serum +0.1% Triton X-100 before adding the primary antibodies solution. Primary antibodies were: rabbit anti-TH (1:1000, Merck Millipore, #AB152), anti-mouse anti-Cre (1:500 ab24607), chicken anti-GFP (1:1000, Abcam, #ab13970). After incubation with primary antibodies overnight at 4 °C, the cells were washed three times before adding fluorophore-conjugated secondary antibodies (1:200, Jackson ImmunoResearch Laboratories) and DAPI (1:500). The cultures were incubated with secondary antibodies for 2 h and finally washed three times.

4.8. Immunohistochemistry

After perfusion, brains were post-fixed for 24 h in 4% PFA and then cryopreserved in a 30% sucrose solution before being sectioned coronally on a freezing sledge microtome at a thickness of 35 μm in series of 1:8 or 1:12.

Immunohistochemistry was performed on free-floating sections and all washing steps were carried out with 0.1 M phosphate buffered saline with potassium (KPBS, pH 7.4). The sections were washed three times and then incubated in Tris-EDTA pH 8 for 30 min at 80 °C for antigen retrieval. After washing an additional three times, the sections were incubated in blocking solution (5% serum, 0.25% Triton X-100) for 1 h, before adding the primary antibody solution. Primary antibodies used were: mouse anti-HuNu (1:200, Merck Millipore, #MAB1281), rabbit anti-TH (1:1000, Merck Millipore, #AB152) and chicken anti-GFP (1:1000, Abcam, #ab13970). After incubation with primary antibodies overnight at room temperature, the sections were washed twice and incubated in blocking solution for 30–45 min. For fluorescent immunolabeling, the sections were then incubated with fluorophore-conjugated secondary antibodies (1:200, Jackson ImmunoResearch Laboratories) for 2 h at room temperature, washed three times and then mounted on gelatin-coated slides and cover-slipped with PVA-DABCO containing DAPI (1:1000).

4.9. Microscopy

Images were captured using either an Epson Perfection V850 PRO flatbed scanner, a Leica DMI6000B widefield microscope, or a Leica TCS SP8 confocal laser scanning microscope. Image acquisition software was Leica LAS X and images were processed using Volocity 6.5.1 software (Quorum Technologies) and Adobe Photoshop. Any adjustments were applied equally across the entire image and without the loss of any information.

4.10. Whole cell patch clamp recordings

Prior to recording, cells on coverslips were transferred to recording chamber containing Krebs solution gassed with 95% O_2 and 5% CO_2 at RT and exchanged every 20 min during recordings. The standard solution was composed of (in mM): 119 NaCl, 2.5 KCl, 1.3 $MgSO_4$, 2.5 $CaCl_2$, 25 glucose, and 26 $NaHCO_3$. For recordings, a Multiclamp 700B Microelectrode Amplifier (Molecular Devices) was used together with borosilicate glass pipettes (3–7 MOhm) filled with the following intracellular solution (in mM): 122.5 potassium gluconate, 12.5 KCl, 0.2 EGTA, 10 HEPES, 2 MgATP, 0.3 Na_3GTP, and 8 NaCl adjusted to pH 7.3 with KOH, as previously described. Data acquisition was performed with pCLAMP 10.2 software (Molecular Devices); current was filtered at 0.1 kHz and digitized at 2 kHz. Cells with neuronal morphology and round cell body were selected for recordings. Resting membrane potentials were monitored immediately after breaking-in in current-clamp mode. Thereafter, cells were kept at a membrane potential of -60 mV to -80 mV, and 500 ms currents were injected from -85 pA to +165 pA with 20 pA increments to induce action potentials. For inward sodium and delayed rectifying potassium current measurements, cells were clamped at -70 mV and voltage-depolarizing steps were delivered for 100 ms at 10 mV increments.

4.11. Statistical analysis

Statistical significance was determined by a two-tailed paired Student's t-test. P-values <0.05 were considered as statistically significant. Error bars represent SEM.

Declarations

Author contribution statement

Fiorenzano A: Conceived and designed the experiments; Performed the experiments; Analyzed and interpreted the data; Wrote the paper.

Marcella Birtele & Nelander Wahlestedt J: Performed the experiments; Analyzed and interpreted the data.

Parmar M: Conceived and designed the experiments; Analyzed and interpreted the data; Contributed reagents, materials, analysis tools or data; Wrote the paper.

Funding statement

This work was supported by the New York Stem Cell Foundation (MP), the European Research Council (ERC Grant Agreement no. 771427, MP), the Swedish Research Council (grant agreements 2016–00873 [MP]), the Swedish Parkinson Foundation (Parkinsonfonden, MP), the Swedish Brain Foundation (Hjärnfonden FO2019-0301, MP), the Strategic Research Area at Lund University MultiPark (Multidisciplinary research in Parkinson's disease) and KAW (2018.0040).

Data availability statement

Data included in article/supp. material/referenced in article.

Declaration of interests statement

The authors declare no conflict of interest.

Additional information

Supplementary content related to this article has been published online at https://doi.org/10.1016/j.heliyon.2021.e06006.

Acknowledgements

We thank Ulla Jarl, Marie Persson Vejgården, and Mikael Sparrenius for technical assistance; Bengt Mattsson for his valuable help with microscopy.

References

[1] R.A. Barker, J. Drouin-Ouellet, M. Parmar, Cell-based therapies for Parkinson disease-past insights and future potential, Nat. Rev. Neurol. 11 (9) (2015) 492–503.
[2] M. Parmar, Towards stem cell based therapies for Parkinson's disease, Development 145 (1) (2018).
[3] R.A. Barker, et al., Human trials of stem cell-derived dopamine neurons for Parkinson's disease: dawn of a new era, Cell Stem Cell 21 (5) (2017) 569–573.
[4] J.S. Schweitzer, et al., Personalized iPSC-derived dopamine progenitor cells for Parkinson's disease, N. Engl. J. Med. 382 (20) (2020) 1926–1932.
[5] J.A. Steinbeck, et al., Optogenetics enables functional analysis of human embryonic stem cell-derived grafts in a Parkinson's disease model, Nat. Biotechnol. 33 (2) (2015) 204–209.
[6] J. Xi, et al., Specification of midbrain dopamine neurons from primate pluripotent stem cells, Stem Cell. 30 (8) (2012) 1655–1663.
[7] P. Aldrin-Kirk, et al., DREADD modulation of transplanted DA neurons reveals a novel parkinsonian dyskinesia mechanism mediated by the serotonin 5-HT6 receptor, Neuron 90 (5) (2016) 955–968.
[8] T. Cardoso, et al., Target-specific forebrain projections and appropriate synaptic inputs of hESC-derived dopamine neurons grafted to the midbrain of parkinsonian rats, J. Comp. Neurol. 526 (13) (2018) 2133–2146.
[9] A.F. Adler, et al., hESC-derived dopaminergic transplants integrate into basal ganglia circuitry in a preclinical model of Parkinson's disease, Cell Rep. 28 (13) (2019) 3462-+.
[10] A.J. Brown, et al., Whole-rat conditional gene knockout via genome editing (vol 10, pg 638, 2013), Nat. Methods 10 (10) (2013) 1035-1035.
[11] H. Taniguchi, et al., A resource of Cre driver lines for genetic targeting of GABAergic neurons in cerebral cortex, Neuron 71 (6) (2011) 995–1013.
[12] A. Kirkeby, et al., Predictive markers guide differentiation to improve graft outcome in clinical translation of hESC-based therapy for Parkinson's disease, Cell Stem Cell 20 (1) (2017) 135–148.
[13] S. Nolbrant, et al., Generation of high-purity human ventral midbrain dopaminergic progenitors for in vitro maturation and intracerebral transplantation, Nat. Protoc. 12 (9) (2017) 1962–1979.
[14] S. Li, et al., Overview of the reporter genes and reporter mouse models, Animal Model Exp Med 1 (1) (2018) 29–35.
[15] K. Tiklova, et al., Single cell transcriptomics identifies stem cell-derived graft composition in a model of Parkinson's disease, Nat. Commun. 11 (1) (2020) 2434.
[16] S. Grealish, et al., Monosynaptic tracing using modified rabies virus reveals early and extensive circuit integration of human embryonic stem cell-derived neurons, Stem Cell Reports 4 (6) (2015) 975–983.
[17] A. Heuer, et al., Dopamine-rich grafts alleviate deficits in contralateral response space induced by extensive dopamine depletion in rats, Exp. Neurol. 247 (2013) 485–495.